Journal of the Geological Society, *London*, Vol. **164**, 2007, pp. 1–13. Printed in Great Britain.

Carboniferous granitic plutons from the northern margin of the North China block: implications for a late Palaeozoic active continental margin

SHUAN-HONG ZHANG[1,2], YUE ZHAO[1], BIAO SONG[2], ZHEN-YU YANG[1], JIAN-MIN HU[1] & HAI WU[3]

[1]*Key Laboratory of Crustal Deformation and Processes, Institute of Geomechanics, Chinese Academy of Geological Sciences, Beijing 100081, China*

[2]*Beijing SHRIMP Centre, Chinese Academy of Geological Sciences, Beijing, 100037, China (e-mail: tozhangshuanhong@163.com)*

[3]*Geological Information Centre, Ministry of Land and Resource, Yanjiao, Hebei Province 065201, China*

Abstract: We report four late Palaeozoic zircon sensitive high-resolution ion microprobe (SHRIMP) U–Pb ages for granitic plutons from the Inner Mongolia Palaeo-uplift on the northern margin of the North China block. These cast a new light on the poorly understood tectonic history of the northern margin of the North China block and the Central Asian Orogenic Belt during the late Palaeozoic. The plutons have for a long time been considered to belong to the early Precambrian basement of the North China block. Our new SHRIMP U–Pb zircon dating of four plutons at Longhua, Daguangding, Boluonuo and Hushiha has yielded intrusive ages of 311 ± 2 Ma, 324 ± 6 Ma, 302 ± 4 Ma and 310 ± 5 Ma, respectively. Geochemical data suggest that these granitoids have a calc-alkaline, subduction-related I-type signature, indicating the existence of an Andean-style continental arc along the northern margin of the North China block during the late Palaeozoic. Our results also indicate that the Palaeo-Asian Ocean still existed during latest Carboniferous–earliest Permian time, and that the final collision between the southern Mongolia composite terranes and the North China block occurred later than *c*. 290 Ma. We suggest that the northern margin of the North China block was an active continental margin and the Inner Mongolia Palaeo-uplift is a deeply exhumed mid-crustal ‘root’ of a late Palaeozoic Andean-style continental arc.

The Central Asian Orogenic Belt has become a hotspot of geological research and has been regarded as the world’s largest site of juvenile crustal formation in the Phanerozoic (Wang & Liu 1986; Sengör *et al*. 1993; Sengör & Natal’in 1996; Jahn *et al*. 2000; Heubeck 2001; Xiao *et al*. 2003). As the southern segment of the Central Asian Orogenic Belt, the Solonker suture leading to the final amalgamation of the North China block and the southern Mongolian composite terranes is of key importance to the Central Asian Orogenic Belt. However, the age and the process of the amalgamation between the North China block and the southern Mongolian composite terranes remain controversial. Some workers believe that the Palaeo-Asian oceanic crust was subducted southward beneath the North China block (e.g. Wang 1996; Davis *et al*. 2001; Xiao *et al*. 2003), whereas others favour the northern margin of the North China block as a passive margin subducting northward beneath successively accreting arc terranes or a continental arc–accretionary complex (Hsu *et al*. 1991; Robinson *et al*. 1999), or no southward subduction of the Palaeo-Asian Ocean underneath the North China block (Xu & Chen 1997; Shi *et al*. 2004), but solid evidence to support these interpretations is still lacking. Early Precambrian (Archaean–Palaeoproterozoic) high-grade metamorphic rocks are extensively and well exposed along the northern margin of the North China block, and have been considered to constitute a palaeo-uplift from Meso-Neoproterozoic to early Triassic time (Inner Mongolia Palaeo-uplift), named the ‘Inner Mongolia Axis’ (Fig. 1; Huang 1945; HBGMR 1989). Little is known about late Palaeozoic tectonic processes prior to the assembly of the North China block with the southern Mongolia composite terranes along the Solonker suture (Sengör & Natal’in 1996; Xiao *et al*. 2003). In this paper, we present sensitive high-resolution ion microprobe (SHRIMP) U–Pb zircon ages and geochemical data for granitic plutons of the Inner Mongolia Palaeo-uplift that provide evidence for an Andean-style continental arc along the northern margin of the North China block in late Palaeozoic time, which is important for understanding the late Palaeozoic tectonic history of the Central Asian Orogenic Belt.

Geological setting and previous work

The Inner Mongolia Palaeo-uplift is located on the northern margin of the North China block, south of the Central Asian Orogenic Belt and north of the Yanshan fold and thrust belt, separated from the latter by the east–west-striking Pingquan–Gubeikou–Chicheng–Shangyi fault (Fig. 1). The Inner Mongolia Palaeo-uplift is a tectonic province with extensive early Precambrian high-grade basement rocks that are unconformably overlain by Jurassic–Cretaceous volcanic and sedimentary rocks.

The North China block includes highly metamorphosed Archaean and Palaeoproterozoic rocks, Meso-Neoproterozoic, and Cambrian–Ordovician marine clastic and carbonate platformal sediments, middle Carboniferous to Triassic fluvial and deltaic sediments, and Jurassic–Cretaceous and younger volcanic and sedimentary rocks. The Mesoproterozoic and younger rocks are widely distributed within the Yanshan fold and thrust belt, and the maximum thickness of the Meso-Neoproterozoic and Lower Palaeozoic strata is *c*. 11.5 km (HBGMR 1989). However, they are almost entirely absent in the Inner Mongolia Palaeo-uplift, except for some Mesoproterozoic sedimentary rocks along a narrow belt of the Fengning–Longhua fault (Figs 1 and 2).

Article number = 05190

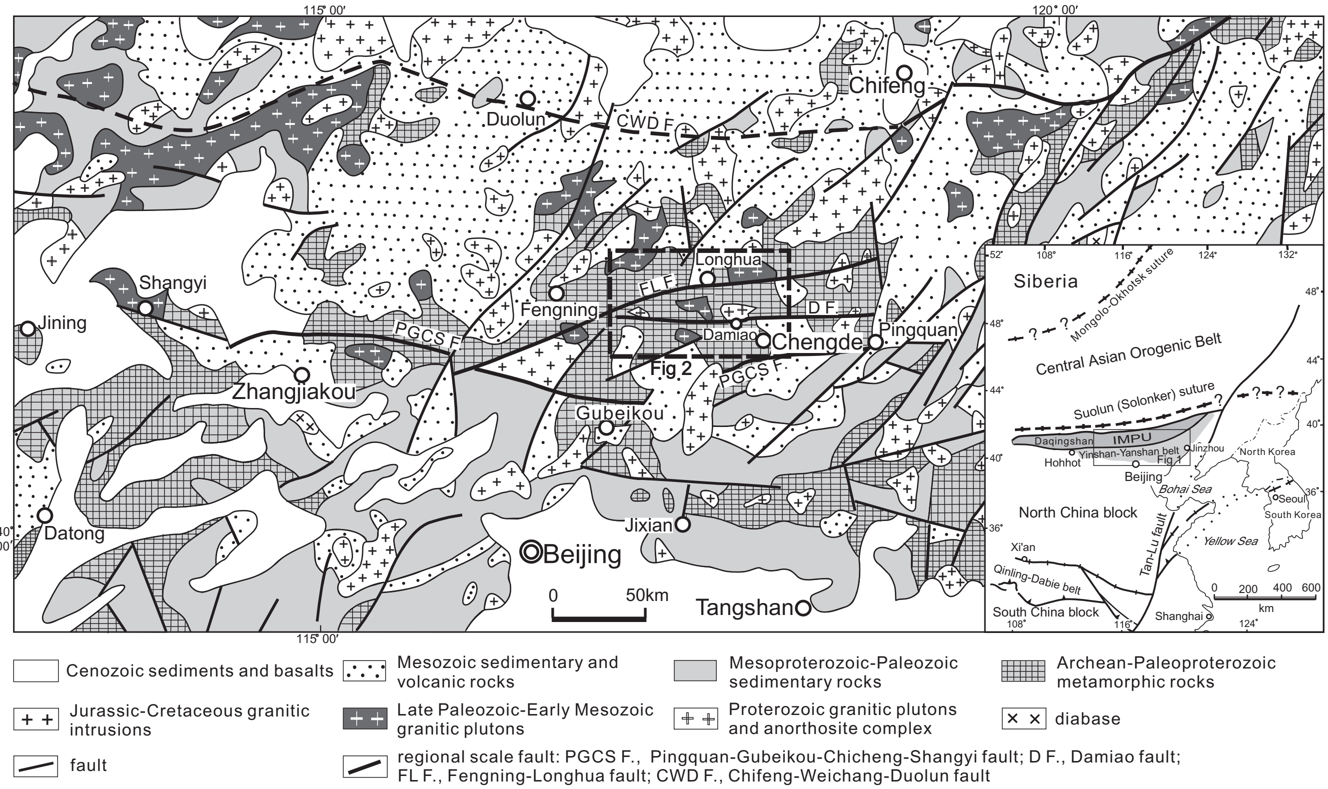

Fig. 1. Geological sketch map of the northern margin of the North China block (modified after HBGMR 1989; LBGMR 1989; Zhang 2004; inset figure modified after Davis *et al*. 2001).

Traditionally, the North China block (including the Inner Mongolia Palaeo-uplift) has been considered stable since the end of rifting in the Neoproterozoic, with no crustal reactivation until the Triassic (Ren *et al*. 1990; Song 1999). Therefore, the possible existence of late Palaeozoic plutons on the northern margin of North China block has been debated for many decades. It has been reported that Permian granitoids exist in northern Hebei Province (HBGMR 1989; Hong *et al*. 1995; Cui & Wu 1997) and western Liaoning Province (LBGMR 1989; Pan 1996) on the northern margin of the North China block, but their accurate ages and petrogenesis are still not clear. Recently, some Permian zircon U–Pb ages were obtained from so-called early Precambrian basement rocks in northern Hebei Province (Kröner *et al*. 2004; and unpubl. data) and from so-called 'Caledonian' granitoids at Yanbian in Jilin Province (Zhang *et al*. 2004), but their petrogenesis is poorly constrained. Late Palaeozoic plutons, commonly overlain unconformably by Jurassic–Cretaceous volcanic and sedimentary rocks, reflect the uplift and exhumation history of the Inner Mongolia Palaeo-uplift and are crucial for understanding its tectonic history and the late Palaeozoic–early Mesozoic history of the northern margin of the North China block and the Central Asian Orogenic Belt.

Field occurrence and sample description

Field occurrence of the investigated plutons

Longhua pluton. The long axis of the Longhua pluton trends east–west, and its area is in excess of 60 km^2. The pluton, which is located on the northern side of the Fengning–Longhua fault (Fig. 2), consists of strongly foliated and partly migmatized quartz diorite, quartz monzodiorite and diorite, which are overlain unconformably by Late Jurassic–Early Cretaceous sedimentary and volcanic rocks to the north, and are intruded into Archaean metamorphic rocks to the SE. Previous studies (HBGMR 1974, 1994*a*) interpreted the pluton as migmatites or migmatized metamorphic diorite of Palaeoproterozoic or earlier age. The diorite is strongly deformed with a NE–SW- to ENE–WSW-trending steep foliation. Its main minerals are plagioclase (An 24–43), quartz, hornblende, biotite and K-feldspar; subordinate minerals are magnetite, titanite, apatite and zircon, and occasional pyroxene and secondary chlorite and epidote. Detailed petrographic descriptions are available online at http://www.geolsoc.org.uk/SUP18258. A hard copy can be obtained from the Society Library.

Daguangding pluton. The Daguangding pluton is located between the Fengning–Longhua and Damiao faults (Fig. 2). It is composed of quartz diorite, diorite and gabbroic diorite. Its long axis trends east–west, and its area is about 200 km^2. The strongly deformed diorite has a well-developed foliation, especially in the western part of the pluton, but the foliation strike and dip are not steady. The host rocks of the pluton are Archaean metamorphic rocks, and it is unconformably overlain on its southeastern side by Late Jurassic–Early Cretaceous strata. It has previously been interpreted as an Archaean (HBGMR 1989), Archaean–Proterozoic (HBGMR 1974), or Palaeoproterozoic (HBGMR 1994*b*) pluton. Its minerals are very similar to those of the Longhua pluton (see the Supplementary Publication).

Boluonuo pluton. The long axis of the pluton trends ENE–WSW, and its area is about 80 km^2 (Fig. 2). The main components are quartz diorite, diorite and granodiorite. Foliation is locally developed, but deformation is less severe than that of the Longhua and Daguangding plutons. As in the case of the Daguangding quartz diorite, this pluton has previously been viewed as Archaean (HBGMR 1989), Archaean–Proterozoic (HBGMR 1974) or Palaeoproterozoic in age (HBGMR 1988). Its main minerals are plagioclase (An 20–30), quartz, hornblende, K-feldspar and biotite;

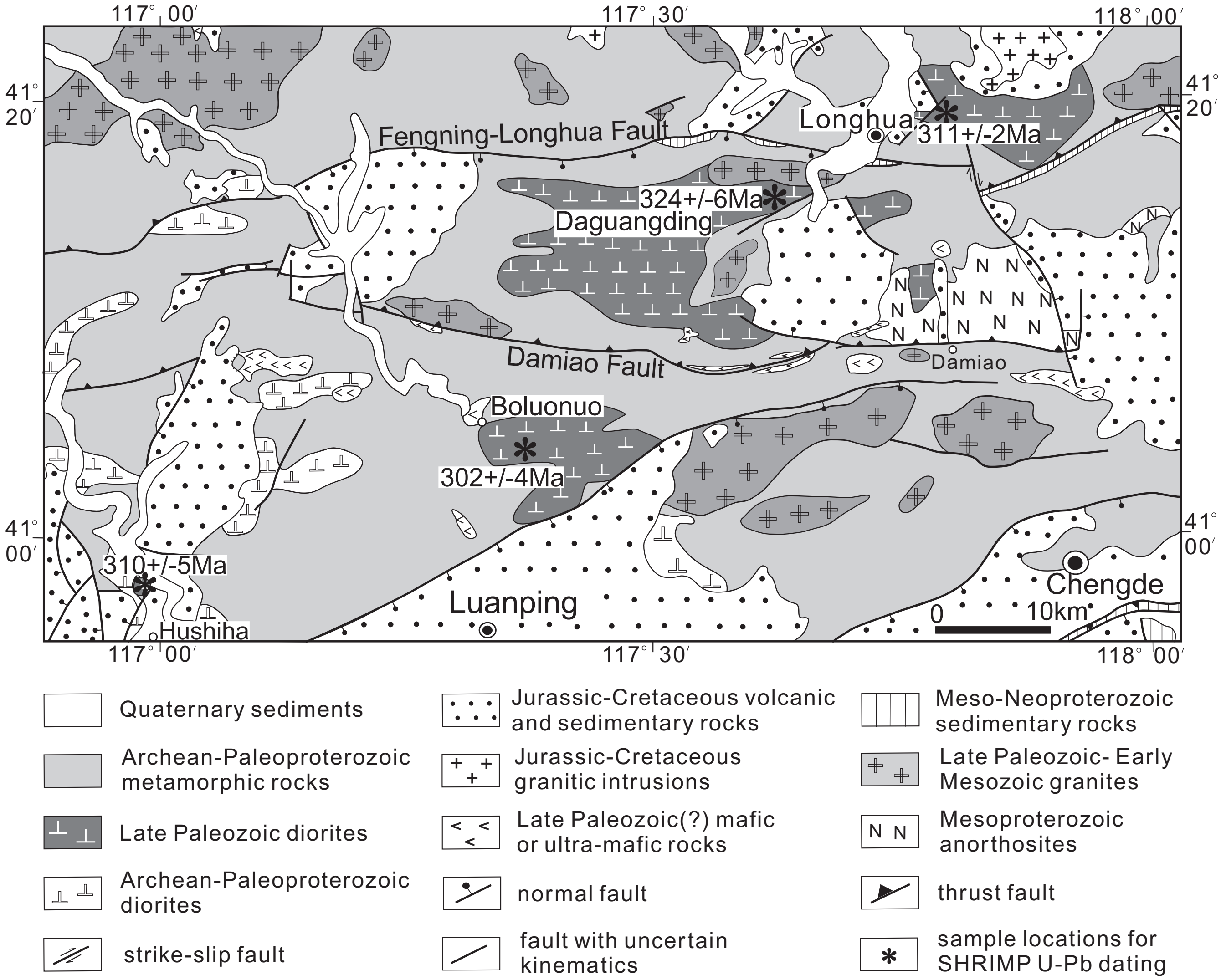

Fig. 2. Geological map of the middle segment of the Inner Mongolia Palaeo-uplift with sampled plutons (modified after HBGMR 1989).

subordinate minerals are magnetite, titanite, apatite and zircon, with secondary chlorite, epidote and sericite (see the Supplementary Publication).

Hushiha pluton. The Hushiha granodiorite is a newly discovered small pluton within Archaean biotite–plagioclase–hornblende gneiss (Fig. 2). Because the outcrop of the pluton is small, it was not shown on previous geological maps (HBGMR 1989). Its main minerals are plagioclase (An *c*. 30), quartz, K-feldspar, biotite and muscovite; subordinate minerals are magnetite, apatite and zircon, with secondary sericite and calcite (see the Supplementary Publication).

Although some rocks of the Carboniferous plutons were foliated, they have not undergone high-grade metamorphism. The secondary chlorite, epidote, sericite or calcite in these rocks is a result of thermal alteration or low-grade metamorphism caused by their deep emplacement. Because contents of the secondary minerals are very low (<1–2 vol%), they have only slight influence on the geochemical compositions of the Carboniferous rocks, and the present geochemical compositions of the plutons are very similar to the original plutonic compositions.

Sample description

Sample SD020-3 is a gneissic quartz diorite from the eastern part of the Longhua pluton (Fig. 2). It is composed of plagioclase (55–60 vol%), quartz (15–20 vol%), hornblende (10–15 vol%), biotite (15–20 vol%) and K-feldspar (1 vol%), with subordinate minerals (<1 vol%) magnetite, titanite, apatite, zircon and allanite, and secondary minerals (<2 vol%) chlorite, epidote and sericite. Zircons are transparent, euhedral, long or short (100–300 μm length) yellowish prisms. Oscillatory zoning is well developed in cathodoluminescence (CL) images, which indicates that the zircon crystals are typically magmatic; some zircons have rounded relict cores (Fig. 3).

Sample D018-1 is a quartz diorite collected from the northeastern part of the Daguangding pluton (Fig. 2). Its main minerals are plagioclase (70–80 vol%), quartz (15–20 vol%), hornblende (3 vol%) and biotite (2 vol%); subordinate minerals (<1 vol%) are magnetite, apatite, titanite, zircon and allanite; secondary minerals (5 vol%) are chlorite, epidote, zoisite and sericite. The zircons are pink, euhedral prisms with oscillatory zoning in CL images, typical of magmatic zircons, some with rounded relict cores (Fig. 3), and the grain size is from 70 to 250 μm.

Sample HLB-G is a quartz diorite from the Boluonuo pluton near a highway south of Boluonuo (Fig. 2). It is composed of plagioclase (70–80 vol%), quartz (5–10 vol%), hornblende (5 vol%), biotite (10–15 vol%), K-feldspar (<5 vol%), and subordinate minerals (<1 vol%) magnetite, apatite and zircon, with secondary minerals (<3 vol%) chlorite, epidote and sericite. The Boluonuo quartz diorite zircons closely resemble those of the Daguangding pluton described above (Fig. 3); the grain size is from 50 to 200 μm.

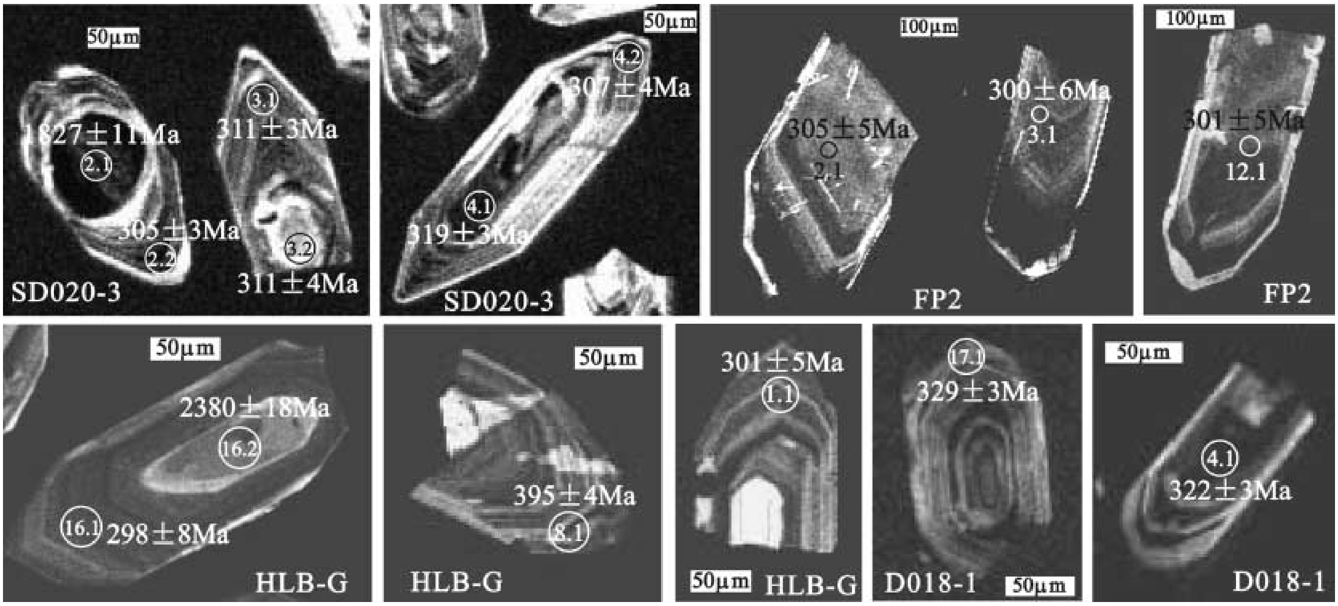

Fig. 3. CL image and dating spots of representative zircons from various samples.

Sample FP2 was collected from the Hushiha granodiorite pluton near a bridge across the Chaohe River, north of Hushiha (Fig. 2). Its main minerals are plagioclase (65–70 vol%), quartz (20 vol%), K-feldspar (5–10 vol%), muscovite (4 vol%) and biotite (1 vol%); subordinate minerals (<1 vol%) are magnetite, apatite and zircon; secondary minerals (2 vol%) are chlorite and sericite. Zircons from the granodiorite are euhedral, long pink prisms that exhibit well-developed magmatic zoning (Fig. 3), and have a grain size from 50 to 300 (m.

More detailed zircon CL images and a summary of all the granitoid samples from the late Palaeozoic plutons are given in the Supplementary Publication.

Methods and analytical procedures

SHRIMP U–Pb dating

Zircons were extracted using conventional separation techniques and were then handpicked under a binocular microscope. Together with the TEMORA zircon standard they were mounted in epoxy and polished to expose the cores of the grains for CL and SHRIMP U–Pb analyses.

U–Pb dating was performed on the SHRIMP II at the Beijing SHRIMP Centre following the method of Williams (1998). The mass resolution was *c.* 5000 at 1% peak height. The spot size of the ion beam was 25–30 µm, and five scans through the mass range were used for data collection. The SL13 (572 Ma, U = 238ppm) and TEMORA (417 Ma) standards were used in the analyses as discussed by Black *et al*. (2003). Sites for dating were selected on the basis of CL and microscope images. To maintain precision, one TEMORA analysis was performed after every three or four spots on the sample zircons during data collection. Ages and concordia diagrams were produced using the programs SQUID 1.03 (Ludwig 2001) and ISOPLOT/Ex 2.06 (Ludwig 1999).

Major and trace element analyses

Fourteen samples (six from the Longhua pluton, four from the Daguangding pluton, three from the Boluonuo pluton and one from the Hushiha pluton) were analysed for major and trace elements at the Key
1 Laboratory of Orogenic Belts and Crustal Evolution in the School of Earth and Space Sciences, Peking University. Major elements were analysed on fused glass discs by X-ray fluorescence spectrometry (XRF) following the method of Harvey (1989). Trace elements (including REE) were analysed by inductively coupled plasma mass spectrometry (ICP-MS) using a VG Axiom multicollector system. Rock powder (0.1 g) was digested with concentrated $HF–HNO_3–HClO_4$ in tightly sealed 15 ml Teflon screw-cap bombs by heating to 110 °C on a hot plate, then evaporating to dryness. The residue was dissolved with 1 ml HNO_3 by heating; subsequently, the final solution was prepared by adding 1% HNO_3 with internal standard and diluted with de-ionized water to 30 ml. An aliquot of 10 ml was taken and also diluted to 30 ml to bring down count rates for detected elements. The composition of the internal standard contains 10 ppb indium to correct for instrumental drift during the ICP-MS analysis; all acids used were ultra-pure. The Chinese national standards GSR-1 were used to monitor analyses. The results of analyses were consistent with the reference values, with the differences for major elements being within 1%, except for P_2O_5 (5%), and trace elements (including REE), which were within 5–10%.

Results

SHRIMP U–Pb dating results

The SHRIMP U–Pb analyses of zircons from the Longhua quartz diorite (sample SD020-3) are listed in Table 1 and plotted on the concordia diagram of Figure 4a. Twenty-six spots on 17 zircon grains were measured, and most are concordant. The errors on spots 1.2 and 8.1 are large because of low U contents. Four rounded cores (2.1, 6.1, 9.1, 12.1) give a $^{207}Pb/^{206}Pb$ mean age of 1809 ± 21 Ma (95% confidence, MSWD = 1.9), and are interpreted as inherited zircons (Fig. 4a inset). Spot 5.1 is rejected because it is far from the concordia curve. Spot 6.2 probably reflects a mixed age of an inherited grain and a magmatic grain because it is near the boundary between the rounded inner core and the magmatic oscillatory overgrowth. Except for these eight anomalous spots, the remaining spots yield a weighted mean $^{206}Pb/^{238}U$ age of 311 ± 2 Ma (95% confidence, MSWD = 2.1, n = 18). Their well-developed oscillatory zoning and high Th/U ratios (>0.4) indicate a magmatic origin. Therefore, the mean age of 311 ± 2 Ma dates the time of crystallization of the Longhua quartz diorite in the late Carboniferious.

For Daguangding quartz diorite sample D018-1, 20 spots on 18 zircon grains were measured, and most are reasonably

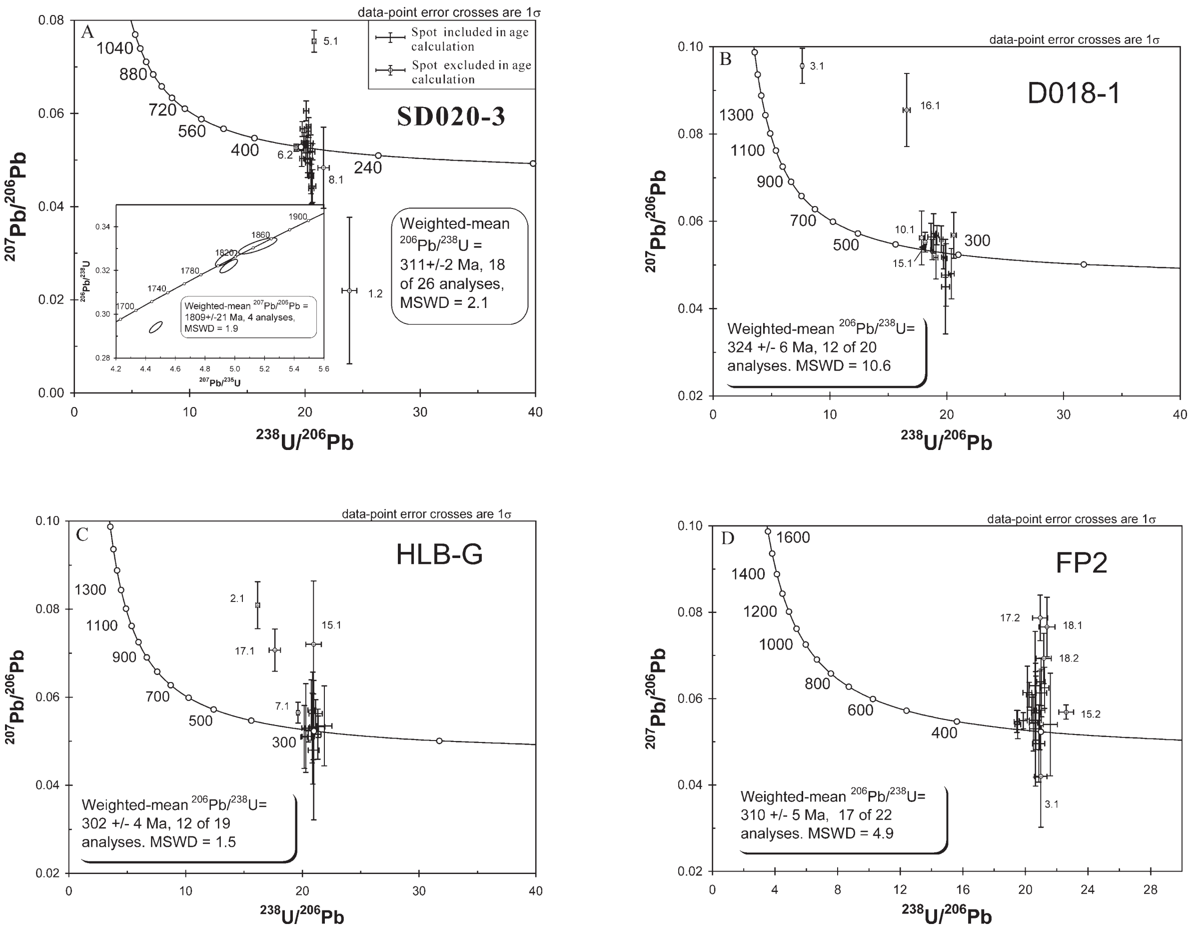

Fig. 4. SHRIMP U–Pb concordia diagram for zircons from various samples: (**a**) sample SD020-3; (**b**) sample D018-1; (**c**) sample HLB-G; (**d**) sample FP2.

concordant (Table 1, Fig. 4b). Eight spots (1.2, 3.1, 10.1, 11.1, 11.2, 15.1, 16.1, 18.1) give inherited or mixed ages between inherited cores and magmatic overgrowth. The remaining spots give a weighted mean $^{206}Pb/^{238}U$ age of 324 ± 6 Ma (95% confidence, MSWD = 10.6, $n = 12$). Although their Th/U ratios are not very high (0.05–0.48, Table 1), their euhedral shape and well-developed oscillatory zoning indicate a magmatic origin. Therefore, 324 ± 6 Ma reflects the crystallization age of the Daguangding pluton.

Nineteen spots on 17 zircon grains from the Boluonuo quartz diorite (sample HLB-G) were measured, and most of them are concordant (Table 1, Fig. 4c). Seven spots (2.1, 7.1, 13.2, 14.1, 15.1, 16.2, 17.1) were rejected because they are not concordant and have lost radiogenic lead. The remaining spots give a weighted mean $^{206}Pb/^{238}U$ age of 302 ± 4 Ma (95% confidence, MSWD = 1.5, $n = 12$), indicating the time of emplacement of the diorite in the late Carboniferous.

Twenty-two spots on 18 zircon grains from the Hushiha granodiorite (sample FP2) were measured, and most of them give concordant ages (Table 1, Fig. 4d). Except for five discordant spots (3.1, 15.2, 17.2, 18.1, 18.2), the spots give a weighted mean $^{206}Pb/^{238}U$ age of 310 ± 5 Ma (95% confidence, MSWD = 4.9, $n = 17$), which we interpret as the emplacement age of the Hushiha granodiorite in the late Carboniferous.

Major and trace element geochemistry

Major element compositions. The major element compositions of the Longhua, Daguangding and Boluonuo plutons are characterized by variable contents of SiO_2, high contents of Al_2O_3, CaO and Na_2O, and high Na_2O/K_2O ratios (Table 2); they have the chemical signatures of I-type granites. The Longhua pluton quartz diorites and quartz monzodiorite tend to have higher contents of TiO_2, TFe_2O_3, MnO, MgO, CaO, K_2O and P_2O_5 than the Daguangding, Boluonuo and Hushiha plutons. The Mg-number values of the plutons range from 34.4 to 47.7. According to the classification of Peccerillo & Taylor (1976), they belong to the calc-alkaline or high-K calc-alkaline series. An A/NK v. A/CNK diagram (not presented) indicates that most of the samples are metaluminous (A/CNK <1 and A/NK >1).

REE compositions. The total REE contents ($\sum$REE) of each pluton are very different, and samples from the Longhua pluton have higher REE contents than those from the Daguangding, Boluonuo and Hushiha plutons. Chondrite-normalized REE patterns are shown in Figure 5 and are characterized by significant heavy REE (HREE) depletion ($La_N/Yb_N = 11.76$–34.34). They show no obvious Eu anomalies or positive Eu anomalies

Table 1. *SHRIMP U–Pb results for the Carboniferous plutons*

Grain-spot	Grain area	$^{206}Pb_c$ (%)	U (ppm)	Th (ppm)	Th/U	$^{206}Pb^*$ (ppm)	$^{204}Pb/^{206}Pb$	$^{207}Pb^*/^{206}Pb^*$	$^{207}Pb^*/^{235}U$	$^{206}Pb^*/^{238}U$	$^{206}Pb/^{238}U$ age (Ma)	$^{207}Pb/^{206}Pb$ age (Ma)
Sample SD020-3 (Longhua quartz diorite)												
1.1	r	0.96	308	286	0.93	13.0	0.00053	0.04660 ± 0.00256	0.3120 ± 0.0175	0.04863 ± 0.00048	306 ± 3	
1.2	r	5.45	55	22	0.40	2.10	0.00298	0.02200 ± 0.01584	0.1270 ± 0.0914	0.04190 ± 0.00109	265 ± 7	
2.1	c	0.07	340	134	0.39	94.1	0.00004	0.11171 ± 0.00066	4.9590 ± 0.0481	0.32200 ± 0.00251	1799 ± 12	1827 ± 11
2.2	r	0.44	335	329	0.98	14.0	0.00024	0.05180 ± 0.00176	0.3460 ± 0.0121	0.04841 ± 0.00048	305 ± 3	
3.1	r	0.90	304	265	0.87	13.0	0.00049	0.04940 ± 0.00217	0.3370 ± 0.0152	0.04941 ± 0.00047	311 ± 3	
3.2	m	0.80	135	87	0.64	5.78	0.00044	0.05310 ± 0.00377	0.3620 ± 0.0261	0.04941 ± 0.00064	311 ± 4	
4.1	m	0.53	404	358	0.89	17.7	0.00029	0.05030 ± 0.00171	0.3520 ± 0.0123	0.05071 ± 0.00045	319 ± 3	
4.2	r	1.20	199	146	0.73	8.41	0.00066	0.04660 ± 0.00382	0.3130 ± 0.0257	0.04871 ± 0.00058	307 ± 4	
5.1	r	2.00	1027	906	0.88	43.3	0.00110	0.07550 ± 0.00234	0.5010 ± 0.0160	0.04808 ± 0.00038	303 ± 2	
6.1	c	0.03	1262	45	0.04	319	0.00002	0.11019 ± 0.00037	4.4680 ± 0.0353	0.29410 ± 0.00209	1662 ± 10	1803 ± 6
6.2	m	0.20	1200	126	0.11	53.7	0.00011	0.05264 ± 0.00074	0.3774 ± 0.0060	0.05200 ± 0.00040	327 ± 2	
6.3	r	0.78	268	148	0.55	11.6	0.00043	0.05270 ± 0.00237	0.3620 ± 0.0170	0.04981 ± 0.00050	313 ± 3	
7.1	m	0.12	178	247	1.39	7.62	0.00007	0.06060 ± 0.00212	0.4150 ± 0.0154	0.04973 ± 0.00055	313 ± 3	
7.2	c	0.09	1332	974	0.73	57.3	0.00005	0.05348 ± 0.00064	0.3687 ± 0.0052	0.05001 ± 0.00038	315 ± 2	
8.1	m	2.61	75	87	1.16	3.07	0.00143	0.04830 ± 0.00869	0.3080 ± 0.0554	0.04630 ± 0.00106	292 ± 7	
9.1	c	0.13	191	125	0.65	53.4	0.00008	0.11009 ± 0.00087	4.9420 ± 0.0593	0.32550 ± 0.00293	1817 ± 14	1801 ± 14
9.2	r	0.40	371	366	0.99	16.2	0.00022	0.05670 ± 0.00159	0.3950 ± 0.0119	0.05060 ± 0.00046	318 ± 3	
10.1	m	1.23	218	166	0.76	9.23	0.00067	0.04390 ± 0.00329	0.2940 ± 0.0223	0.04861 ± 0.00053	306 ± 3	
11.1	m	0.55	176	192	1.09	7.63	0.00030	0.05370 ± 0.00220	0.3720 ± 0.0156	0.05023 ± 0.00060	316 ± 4	
12.1	c	0.18	176	61	0.35	50.1	0.00011	0.11290 ± 0.00203	5.1500 ± 0.1082	0.33120 ± 0.00301	1844 ± 15	1846 ± 33
12.2	r	0.65	880	745	0.85	37.5	0.00035	0.05620 ± 0.00135	0.3810 ± 0.0103	0.04923 ± 0.00054	310 ± 3	
13.1	m	0.72	470	541	1.15	19.9	0.00039	0.04930 ± 0.00232	0.3330 ± 0.0157	0.04900 ± 0.00044	308 ± 3	
14.1	m	0.32	189	116	0.61	7.93	0.00017	0.05370 ± 0.00172	0.3610 ± 0.0123	0.04880 ± 0.00054	307 ± 3	
15.1	m/r	–	232	287	1.24	9.80	0.00006	0.05720 ± 0.00189	0.3880 ± 0.0132	0.04922 ± 0.00049	310 ± 3	
16.1	m/r	1.02	173	164	0.95	7.41	0.00056	0.05020 ± 0.00392	0.3420 ± 0.0267	0.04944 ± 0.00059	311 ± 4	
17.1	m	1.35	192	155	0.81	8.09	0.00074	0.04440 ± 0.00351	0.2970 ± 0.0238	0.04843 ± 0.00068	305 ± 4	
Sample D018-1 (Daguangding quartz diorite)												
1.1	r	2.07	338	16	0.05	14.9	0.00114	0.04770 ± 0.00716	0.3300 ± 0.0495	0.05016 ± 0.00095	316 ± 6	
1.2	m/c	1.23	233	81	0.35	23.9	0.00070	0.12640 ± 0.00367	2.0530 ± 0.0657	0.11780 ± 0.00153	718 ± 9	2048 ± 52
2.1	r	2.79	334	136	0.41	14.8	0.00153	0.04500 ± 0.01080	0.3090 ± 0.0742	0.05026 ± 0.00085	316 ± 5	
3.1	r/m	0.95	237	57	0.24	27.0	0.00054	0.09560 ± 0.00402	1.7280 ± 0.0743	0.13110 ± 0.00131	794 ± 8	1540 ± 79
4.1	m	0.66	578	173	0.30	25.6	0.00036	0.05590 ± 0.00302	0.3950 ± 0.0217	0.05121 ± 0.00041	322 ± 3	
5.1	m/c	1.27	368	72	0.20	15.6	0.00070	0.05680 ± 0.00523	0.3800 ± 0.0353	0.04855 ± 0.00053	306 ± 3	
6.1	r	0.49	1483	402	0.27	68.3	0.00027	0.05350 ± 0.00230	0.3940 ± 0.0169	0.05334 ± 0.00034	335 ± 2	
7.1	r	0.94	469	147	0.31	21.8	0.00052	0.05640 ± 0.00316	0.4170 ± 0.0242	0.05363 ± 0.00075	337 ± 4	
8.1	r	1.97	680	158	0.23	30.0	0.00108	0.05150 ± 0.00433	0.3580 ± 0.0304	0.05033 ± 0.00044	317 ± 3	
9.1	r	1.63	416	105	0.25	19.3	0.00090	0.05720 ± 0.00452	0.4180 ± 0.0334	0.05300 ± 0.00053	333 ± 3	
10.1	r	3.02	735	142	0.19	36.5	0.00166	0.05620 ± 0.00618	0.4340 ± 0.0521	0.05603 ± 0.00062	351 ± 4	
11.1	r/c	4.53	603	64	0.11	38.8	0.00252	0.13130 ± 0.00722	1.2950 ± 0.0738	0.07152 ± 0.00086	445 ± 5	2115 ± 97
11.2	c	0.15	1167	207	0.18	350	0.00010	0.15424 ± 0.00065	7.4090 ± 0.0467	0.34840 ± 0.00160	1927 ± 8	2394 ± 7
12.1	r	2.14	311	54	0.17	13.4	0.00117	0.04800 ± 0.00576	0.3240 ± 0.0389	0.04899 ± 0.00059	308 ± 4	
13.1	m	1.11	629	74	0.12	27.7	0.00061	0.05180 ± 0.00269	0.3620 ± 0.0192	0.05068 ± 0.00044	319 ± 3	
14.1	r	0.75	776	216	0.28	35.1	0.00041	0.05680 ± 0.00222	0.4090 ± 0.0160	0.05223 ± 0.00038	328 ± 2	
15.1	r	1.03	1178	122	0.10	56.3	0.00057	0.05520 ± 0.00226	0.4190 ± 0.0176	0.05511 ± 0.00040	346 ± 2	
16.1	r/m	3.30	157	24	0.15	8.40	0.00182	0.08550 ± 0.00838	0.7110 ± 0.0711	0.06030 ± 0.00109	378 ± 7	
17.1	r	2.32	554	265	0.48	25.6	0.00128	0.05170 ± 0.00491	0.3740 ± 0.0355	0.05243 ± 0.00051	329 ± 3	
18.1	r/m	0.61	306	96	0.31	92.1	0.00040	0.16530 ± 0.00248	7.9300 ± 0.1348	0.34820 ± 0.00286	1926 ± 14	2510 ± 26

Sample HLB-G (Boluonuo quartz diorite)												
1.1	r	3.19	198	36	0.18	8.42	0.00175	0.05300 ± 0.01272	0.3470 ± 0.0833	0.04788 ± 0.00086	301 ± 5	
2.1	r/m	1.14	361	48	0.13	19.4	0.00063	0.08090 ± 0.00534	0.6900 ± 0.0462	0.06186 ± 0.00062	387 ± 4	
3.1	r	2.29	209	24	0.11	8.78	0.00125	0.05330 ± 0.00746	0.3510 ± 0.0491	0.04777 ± 0.00072	301 ± 4	
4.1	r	2.14	198	19	0.10	8.34	0.00118	0.05300 ± 0.00795	0.3510 ± 0.0562	0.04800 ± 0.00130	302 ± 8	
5.1	r	2.79	159	14	0.09	6.93	0.00153	0.05300 ± 0.01007	0.3610 ± 0.0686	0.04929 ± 0.00084	310 ± 5	
6.1	r	5.62	158	58	0.37	6.85	0.00308	0.04800 ± 0.01584	0.3170 ± 0.1056	0.04770 ± 0.00105	300 ± 6	
7.1	r/m	1.29	1419	147	0.10	62.9	0.00071	0.05650 ± 0.00237	0.3970 ± 0.0167	0.05093 ± 0.00031	320 ± 2	
8.1	r	2.23	566	99	0.17	23.3	0.00122	0.05160 ± 0.00568	0.3340 ± 0.0367	0.04690 ± 0.00061	295 ± 4	
9.1	r	2.71	213	112	0.53	9.06	0.00149	0.05710 ± 0.00685	0.3790 ± 0.0455	0.04817 ± 0.00067	303 ± 4	
10.1	r	2.33	243	28	0.12	10.6	0.00128	0.05100 ± 0.00714	0.3490 ± 0.0489	0.04960 ± 0.00069	312 ± 4	
11.1	r	0.60	2195	119	0.05	92.5	0.00033	0.05110 ± 0.00123	0.3440 ± 0.0124	0.04880 ± 0.00127	307 ± 8	
12.1	r	1.67	395	24	0.06	15.8	0.00091	0.05350 ± 0.00910	0.3370 ± 0.0573	0.04570 ± 0.00137	288 ± 8	
13.1	r	1.06	1456	97	0.07	59.2	0.00058	0.05330 ± 0.00245	0.3440 ± 0.0182	0.04680 ± 0.00122	295 ± 8	
13.2	c	0.13	355	118	0.33	123	0.00009	0.15980 ± 0.00208	8.8700 ± 0.2661	0.40300 ± 0.01088	2181 ± 49	2454 ± 22
14.1	r	0.39	264	71	0.27	79.2	0.00026	0.15150 ± 0.00167	7.2700 ± 0.2108	0.34820 ± 0.00940	1926 ± 45	2363 ± 19
15.1	r	6.02	185	16	0.09	8.05	0.00330	0.07200 ± 0.01440	0.4750 ± 0.0950	0.04770 ± 0.00153	300 ± 9	
16.1	r	0.53	871	25	0.03	35.6	0.00029	0.05630 ± 0.00315	0.3670 ± 0.0228	0.04730 ± 0.00128	298 ± 8	
16.2	c	0.41	199	62	0.31	63.2	0.00027	0.15310 ± 0.00153	7.7600 ± 0.2250	0.36800 ± 0.00994	2019 ± 47	2380 ± 18
17.1	r	0.94	324	38	0.12	15.9	0.00052	0.07070 ± 0.00481	0.5520 ± 0.0403	0.05670 ± 0.00159	355 ± 10	
Sample FP2 (Hushiha granodiorite)												
1.1	m	3.87	128	32	0.25	5.29	0.00212	0.05400 ± 0.01188	0.3420 ± 0.0787	0.04632 ± 0.00097	292 ± 6	
2.1	m	2.83	150	42	0.28	6.43	0.00155	0.05300 ± 0.01325	0.3530 ± 0.0883	0.04845 ± 0.00087	305 ± 5	
3.1	m	3.62	147	46	0.31	6.25	0.00199	0.04200 ± 0.01176	0.2740 ± 0.0767	0.04766 ± 0.00091	300 ± 6	
4.1	m	2.65	161	51	0.32	6.81	0.00145	0.04960 ± 0.00893	0.3280 ± 0.0590	0.04799 ± 0.00091	302 ± 6	
5.1	m	0.80	534	417	0.78	23.8	0.00044	0.05470 ± 0.00257	0.3880 ± 0.0186	0.05141 ± 0.00045	323 ± 3	
6.1	m/r	1.08	442	42	0.10	19.7	0.00059	0.05400 ± 0.00324	0.3820 ± 0.0233	0.05126 ± 0.00049	322 ± 3	
6.2	m	0.35	284	133	0.47	12.3	0.00019	0.05490 ± 0.00187	0.3810 ± 0.0141	0.05035 ± 0.00065	317 ± 4	
7.1	m	1.60	200	56	0.28	8.70	0.00088	0.06140 ± 0.00614	0.4210 ± 0.0421	0.04970 ± 0.00070	313 ± 4	
8.1	r	3.32	159	45	0.28	6.84	0.00182	0.05500 ± 0.01320	0.3700 ± 0.0888	0.04845 ± 0.00087	305 ± 5	
9.1	r/m	1.98	268	162	0.60	11.4	0.00109	0.05440 ± 0.00653	0.3660 ± 0.0439	0.04875 ± 0.00063	307 ± 4	
10.1	m	2.41	163	44	0.27	6.94	0.00132	0.06300 ± 0.01260	0.4180 ± 0.0836	0.04850 ± 0.00087	305 ± 5	
11.1	m	2.28	275	124	0.45	11.7	0.00125	0.05670 ± 0.00851	0.3780 ± 0.0567	0.04838 ± 0.00068	305 ± 4	
12.1	m	2.09	208	64	0.31	8.72	0.00115	0.05730 ± 0.00917	0.3780 ± 0.0605	0.04782 ± 0.00077	301 ± 5	
13.1	m	0.98	335	213	0.64	14.2	0.00054	0.05730 ± 0.00304	0.3870 ± 0.0213	0.04900 ± 0.00069	308 ± 4	
14.1	m	1.21	202	58	0.29	8.36	0.00066	0.06390 ± 0.00550	0.4190 ± 0.0365	0.04762 ± 0.00062	300 ± 4	
15.1	m	1.35	196	65	0.33	8.05	0.00074	0.06250 ± 0.00475	0.4060 ± 0.0313	0.04712 ± 0.00061	297 ± 4	
15.2	r	0.05	904	347	0.38	34.4	0.00003	0.05690 ± 0.00165	0.3470 ± 0.0125	0.04424 ± 0.00093	279 ± 6	
16.1	r/m	0.93	132	26	0.20	5.46	0.00051	0.06130 ± 0.00552	0.4020 ± 0.0366	0.04758 ± 0.00076	300 ± 5	
17.1	m	0.45	431	61	0.14	18.4	0.00025	0.06090 ± 0.00286	0.4150 ± 0.0199	0.04941 ± 0.00045	311 ± 3	
17.2	m	0.00	208	72	0.35	8.52	0.00000	0.07870 ± 0.00527	0.5180 ± 0.0368	0.04770 ± 0.00110	301 ± 7	
18.1	m	0.43	148	43	0.29	5.99	0.00024	0.07660 ± 0.00689	0.4940 ± 0.0459	0.04680 ± 0.00112	295 ± 7	
18.2	m/r	0.46	316	53	0.17	12.9	0.00025	0.06930 ± 0.00582	0.4510 ± 0.0392	0.04720 ± 0.00109	298 ± 7	

All errors are 1σ; $^{206}Pb_c$ (%) indicates the common portions in total ^{206}Pb; $^{206}Pb^*$ refers to the radiogenic ^{206}Pb; common Pb corrected with $^{208}Pb/^{206}Pb = 2.097$, $^{207}Pb/^{206}Pb = 0.864$, $^{206}Pb/^{204}Pb = 18.052$. Grain area as interpreted from CL images; c, core (rounded core usually is discordant with mantle or rim); m, mantle (area between core and rim without clear oscillatory zones); r, rim (usually with oscillatory zones)

Table 2. *Major and trace element compositions of the granitic plutons*

Number:	SD020-3	SD020-1	D017-1	D026-1	D034-1	D036-1	D018-1	D019-1	D159-1	D169-2	HLB-G	D091-1	D097-1	FP2
Location:	LH	LH	LH	LH	LH	LH	DGD	DGD	DGD	DGD	BLN	BLN	BLN	HSH
Major element oxides (wt%)														
SiO_2	61.32	58.01	57.24	56.33	57.72	56.86	66.71	68.60	62.60	63.06	67.70	63.10	66.82	69.34
TiO_2	0.60	0.68	0.92	0.71	0.47	0.48	0.14	0.12	0.60	0.62	0.17	0.40	0.30	0.09
Al_2O_3	17.69	17.83	17.05	17.08	18.85	18.86	18.62	18.09	17.98	17.34	17.37	18.52	16.98	15.86
TFe_2O_3	5.71	6.45	7.61	7.13	5.76	6.62	1.37	1.09	4.61	4.70	2.04	3.79	2.75	0.76
MnO	0.11	0.12	0.12	0.10	0.14	0.15	0.04	0.04	0.07	0.07	0.04	0.07	0.05	0.01
MgO	2.09	2.55	3.51	2.95	1.78	1.97	0.43	0.45	1.77	1.79	0.76	1.50	1.06	0.20
CaO	5.86	5.57	5.75	5.54	5.13	5.21	3.16	2.64	4.80	4.79	3.06	4.08	2.83	1.72
Na_2O	3.74	3.55	3.15	4.30	5.33	6.63	6.63	5.87	4.93	4.78	6.26	5.83	5.03	5.86
K_2O	2.00	2.87	2.27	2.34	4.44	2.67	1.81	2.06	1.61	1.49	1.38	1.93	3.09	2.73
P_2O_5	0.27	0.33	0.27	0.34	0.33	0.36	0.07	0.05	0.25	0.27	0.07	0.22	0.16	0.03
LOI	0.79	2.20	2.19	3.33	0.32	0.51	1.11	1.09	0.50	0.55	1.09	0.56	0.90	3.36
Total	100.18	100.15	100.08	100.15	100.27	100.32	100.09	100.10	99.72	99.46	99.94	100.00	99.97	99.96
A/CNK	0.93	0.93	0.94	0.87	0.82	0.81	1.00	1.08	0.97	0.95	1.00	0.97	1.01	1.01
Na_2O/K_2O	1.87	1.24	1.39	1.84	1.20	2.48	3.66	2.85	3.06	3.21	4.54	3.02	1.63	2.15
CaO/Na_2O	1.57	1.57	1.83	1.29	0.96	0.79	0.48	0.45	0.97	1.00	0.49	0.70	0.56	0.29
Al_2O_3/TiO_2	29.5	26.2	18.5	24.1	40.1	39.3	133.0	150.8	30.0	28.0	102.2	46.3	56.6	176.2
Mg-no.	42.0	43.9	47.7	45.0	38.0	37.1	38.4	45.0	43.3	43.0	42.4	44.0	43.2	34.4
Rare earth elements (ppm)														
La	55.12	58.08	42.12	40.56	50.84	44.76	15.36	16.71	26.58	22.47	18.80	24.75	14.11	10.04
Ce	99.96	109.61	83.18	88.34	86.32	80.65	26.69	29.29	47.71	39.74	33.05	42.50	26.50	17.37
Pr	11.26	12.59	11.92	9.89	11.93	11.14	2.56	3.26	5.58	4.96	3.59	5.09	3.15	1.93
Nd	41.23	47.57	39.56	35.82	42.59	37.37	8.58	12.59	21.58	20.31	12.59	24.41	12.63	6.93
Sm	8.47	7.58	7.78	8.16	8.12	7.34	1.94	2.72	3.15	3.33	2.78	2.95	1.96	0.93
Eu	1.87	2.02	2.09	1.92	2.40	2.37	0.77	1.18	1.37	1.57	1.19	1.16	0.97	0.59
Gd	5.97	6.48	6.81	4.83	6.34	5.27	1.38	1.61	2.61	2.86	1.63	2.43	1.73	0.77
Tb	0.75	0.82	0.99	0.62	0.80	0.71	0.17	0.22	0.34	0.39	0.17	0.29	0.21	0.08
Dy	3.36	3.92	5.02	2.73	3.69	3.26	0.78	1.05	1.64	1.90	0.76	1.44	1.08	0.39
Ho	0.64	0.74	0.95	0.51	0.69	0.63	0.14	0.20	0.29	0.35	0.14	0.26	0.20	0.07
Er	1.85	2.24	2.83	1.49	1.93	1.81	0.43	0.57	0.80	0.95	0.40	0.75	0.58	0.22
Tm	0.24	0.29	0.37	0.20	0.24	0.23	0.06	0.08	0.10	0.12	0.05	0.10	0.08	0.03
Yb	1.54	1.90	2.42	1.34	1.58	1.50	0.44	0.59	0.69	0.82	0.37	0.70	0.58	0.25
Lu	0.23	0.29	0.35	0.19	0.23	0.22	0.07	0.09	0.10	0.12	0.05	0.11	0.09	0.04
$\sum$REE	232.49	254.13	206.39	196.60	217.70	197.26	59.37	70.16	112.54	99.90	75.57	106.95	63.89	39.64
La_N/Yb_N	24.19	20.66	11.76	20.45	21.74	20.16	23.59	19.14	26.03	18.52	34.34	23.89	16.44	27.14
Eu_N/Eu_N(	0.80	0.88	0.88	0.93	1.02	1.16	1.44	1.72	1.46	1.55	1.71	1.32	1.61	2.13

Trace elements (ppm)														
Li	46.35	45.02	28.07	40.02	28.86	18.36	12.90	50.52	6.63	6.19	24.33	8.81	8.40	8.36
Be	1.56	1.44	1.51	1.05	1.69	1.69	1.76	1.21	0.73	0.62	1.04	0.84	0.77	0.66
Sc	9.03	12.12	17.78	11.75	6.85	8.34	3.05	3.16	6.62	7.88	4.00	6.11	4.34	0.85
Co	12.76	13.54	18.70	17.11	14.07	15.24	2.34	2.69	9.88	10.84	4.31	7.29	4.73	1.05
As	2.83	2.67	2.52	2.29	2.67	2.72	2.73	2.70	n.a	n.a	2.30	n.a	n.a	n.a
Cu	2.89	3.68	5.53	3.44	7.07	5.64	4.39	2.54	2.21	2.84	2.40	2.69	3.87	1.70
Ga	32.11	30.96	30.87	28.65	39.96	44.03	23.58	30.50	19.04	18.84	30.94	18.05	16.14	12.25
Rb	44.17	70.17	62.80	53.24	47.48	34.66	29.90	23.42	14.13	14.61	27.08	25.06	32.51	22.89
Sr	859.50	776.91	603.91	815.38	1542.1	1415.3	914.03	967.63	1211.6	1147.0	1215.1	1751.0	1259.0	917.9
Y	23.49	24.64	27.60	18.55	23.56	23.11	10.55	5.28	6.90	8.13	8.44	6.54	5.17	1.98
Zr	99.64	95.94	58.40	77.28	65.91	70.25	81.99	81.35	100.08	105.78	46.23	112.42	90.05	40.85
Nb	14.46	7.82	18.36	14.24	6.67	14.69	6.87	9.13	4.26	4.49	8.51	6.10	4.60	4.26
Ba	1051.5	1089.0	982.34	895.2	1607.8	2008.7	432.87	1035.4	1279.2	1017.3	1240.6	1677.8	2845.4	2892.4
Hf	2.44	2.42	1.50	1.94	1.38	1.85	2.11	2.20	3.33	3.55	0.93	3.50	3.04	1.43
Ta	0.31	0.44	0.48	0.18	0.20	0.27	0.22	0.31	0.20	0.20	0.15	0.24	0.26	0.20
Pb	16.40	17.49	15.86	15.16	22.36	18.29	15.48	16.76	5.18	4.87	19.07	15.12	20.91	19.37
Th	7.21	8.44	5.86	5.96	4.55	5.18	1.55	2.63	2.43	2.15	0.56	2.49	1.32	3.06
U	0.50	0.45	0.28	0.21	0.05	0.44	0.33	0.37	0.63	0.42	0.16	0.34	0.47	0.22
Rb/Sr	0.051	0.090	0.104	0.065	0.031	0.024	0.033	0.024	0.012	0.013	0.022	0.014	0.026	0.025
Rb/Ba	0.042	0.064	0.064	0.059	0.030	0.017	0.069	0.023	0.011	0.014	0.022	0.015	0.011	0.008
Rb/Zr	0.443	0.731	1.075	0.689	0.720	0.493	0.365	0.288	0.141	0.138	0.586	0.223	0.361	0.560
Th/Ta	23.26	19.18	12.21	33.11	22.75	19.19	7.05	8.48	12.15	10.75	3.73	10.38	5.08	15.30
Sr/Y	36.59	31.53	21.88	43.96	65.45	61.24	86.64	183.26	175.52	141.07	143.97	267.90	243.33	464.52

LH, Longhua pluton; DGD, Daguangding pluton; BLN, Boluonuo pluton; HSH, Hushiha pluton. TFe_2O_3, Fe_2O_3 total; LOI, loss on ignition; A/CNK = molecular$Al_2O_3/(CaO + Na_2O + K_2O)$; Mg – number = molecularTFeO/(TFeO + MgO); Eu_N, chondrite-normalized Eu; $Eu_N(= (Sm_N \times Gd_N)^{1/2}$; n.a., not analysed.

(Fig. 5), indicating absence of plagioclase in the melting residue. Such REE characteristics are similar to those of adakitic rocks and arc magmatism (e.g. Defant & Drummond 1990; Drummond *et al*. 1996; Martin 1999; Smithies 2000; Zhou *et al*. 2002; Martin *et al*. 2005).

Trace element compositions. The trace element compositions of all the plutons are broadly similar, with constant low Rb/Sr and Rb/Ba values (Table 2). On primitive mantle-normalized diagrams (Fig. 6), all samples display a moderate to strong depletion in P, Nb, Ta and Ti, which is a characteristic feature shared by many subduction-related magmatic rocks (Briqueu *et al*. 1984; Rogers & Hawkesworth 1989; Sajona *et al*. 1996; Chen *et al*. 2000; Zhou *et al*. 2002). They also have high Th/Ta ratios (3.37–33.11), which is again indicative of subduction-related magmas (Rogers & Hawkesworth 1989; Chen *et al*. 2000; Gorton & Schandl 2000). On Sr/Y v. Y and La_N/Yb_N v. Yb_N diagrams, the Daguangding, Boluonuo and Hushiha plutons have an adakitic composition, and the Longhua pluton has the composition of tholeiitic and calc-alkaline island-arc rocks (Fig. 7).

The Rb, Nb and Y contents of all samples are low. In the tectonic discrimination diagrams of Pearce *et al*. (1984), they all fall in the VAG (volcanic-arc granitoids) field (Fig. 8a and b). On the ternary tectonic discrimination diagram of Harris *et al*. (1986), most samples also fall in or close to the VAG field (Fig. 8c). For magmatic arc granitoids, a diagram of Rb/Zr v. Nb can be used as a qualitative indicator of arc maturity (Brown *et al*. 1984). Most samples fall within the field of normal continental arcs, or near the boundary between primitive arcs and normal continental arcs (Fig. 8d). Therefore, we interpret these rocks as having formed in a primitive–normal continental magmatic arc environment that was probably related to southward subduction of the Palaeo-Asian oceanic crust beneath the North China block.

Discussion

Tectonic setting of the granitic plutons

Our new SHRIMP zircon ages indicate that the Longhua, Daguangding, Boluonuo and Hushiha plutons are late Palaeozoic in age, and not Archaean or Palaeoproterozoic as previously thought (e.g. HBGMR 1989, 1994*a*, *b*). They were intruded into the basement of the North China block during Carboniferous time. Geochemical analyses indicate that the Carboniferous plutons are calc-alkaline, I-type granitoids that show features of subduction-related magmatism. Our recent field investigation and lithological comparison indicate that this type of dioritic plutons may occur widely in the area to the east and west of these four investigated plutons, which together form a Carboniferous arc magmatic belt in the Inner Mongolia Palaeo-uplift along the northern margin of the North China block.

Tuff layers in Upper Palaeozoic sedimentary rocks are widely distributed near Daqingshan, Datong, Tangshan, western Beijing and Jinzhou in the North China block (e.g. Zhong *et al*. 1995; Jia *et al*. 1999; Zhou *et al*. 2001). Geochemical analyses of the tuffs indicate they have a calc-alkaline, volcanic arc composition (Jia *et al*. 1999). Sedimentary and tectonic analysis indicates a northern provenance (e.g. Zhong *et al*. 1995; Jia *et al*. 1999), specifically the northern margin of the North China block and especially the Inner Mongolia Palaeo-uplift. Therefore, these tuffs may record volcanic activity at the northern margin of the North China block in late Palaeozoic time.

SHRIMP zircon dating of a tuff layer from western Beijing

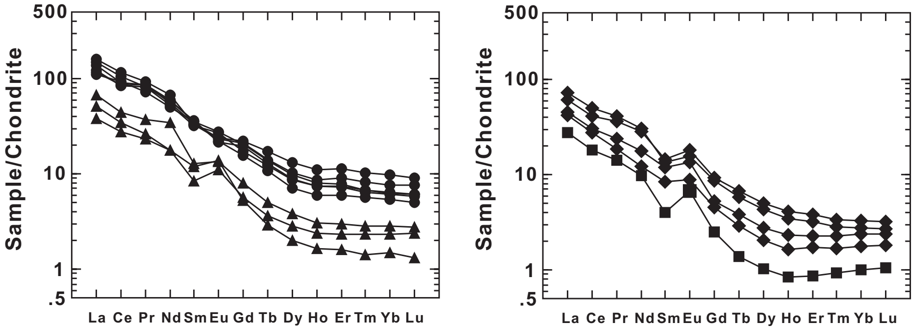

Fig. 5. Chondrite-normalized REE patterns of the granitic plutons. The chondrite values are from Taylor & McLennan (1985). ●, Longhua diorite; ♦, Daguangding diorite; ▲, Boluonuo diorite; ■, Hushiha granite.

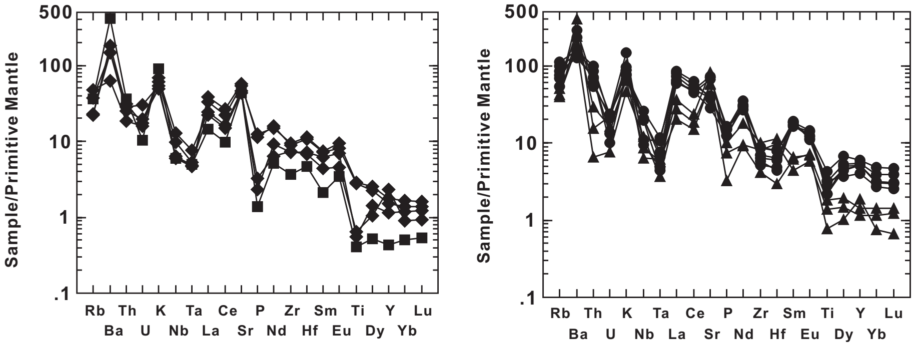

Fig. 6. Primitive mantle-normalized spider diagrams of the granitic plutons. The primitive mantle values are from Sun & McDonough (1989). Symbols are in as Figure 5.

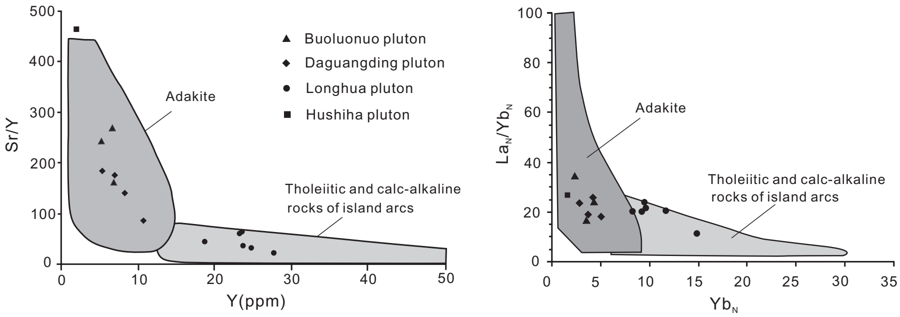

Fig. 7. Sr/Y v. Y and La_N/Yb_N v. Yb_N diagrams for the granitic plutons and adakite assemblages. The chondrite values are from Evensen *et al.* (1978); the fields of island-arc volcanics and adakites in the Sr/Y v. Y diagram are after Martin (1999); the fields of island-arc volcanic rocks and adakites in the La_N/Yb_N v. Yb_N diagram are after Drummond & Defant (1990).

(sample T3S-1, GPS position: 115°55′29.6″; 39°56′57.3″) yielded a $^{206}Pb/^{238}U$ weighted mean age of 296 ± 4 Ma (95% confidence, MSWD = 3.3, $n = 14$; Zhang 2004). And an ash sample from the Upper Palaeozoic sequence near Daqingshan (Fig. 1 inset) also yielded a SHRIMP U–Pb concordia age of 290 ± 6 Ma (Cope *et al.* 2005), which is similar to the volcanic tuff age obtained from western Beijing. These indicate volcanic activity during the latest Carboniferous to earliest Permian, presumably in the northern North China block and the Inner Mongolia Palaeo-uplift, where there are granitic plutons of comparable age as documented above. The presence of volcanic clasts or cobbles (mainly andesite) in the lower parts of a late Triassic(?) conglomeratic sequence of the Xingshikou Formation in northern Hebei Province (Davis *et al.* 2001) and western Beijing is supporting evidence for the existence of volcanic rocks in the Inner Mongolia Palaeo-uplift on the northern margin of the North China block during the late Palaeozoic to early Mesozoic time.

We suggest that the Carboniferous granitoid plutons and latest Carboniferous–earliest Permian volcanic rocks resulted from southward subduction of the Palaeo-Asian oceanic lithosphere beneath the northern margin of the North China block. The existence of late Palaeozoic magmatic arc plutons and possible arc volcanic rocks demonstrates that the northern margin of the North China block was an active continental margin (e.g. Wang 1996; Davis *et al.* 2001; Xiao *et al.* 2003) instead of a passive continental margin (e.g. Xu & Chen 1997; Shi *et al.* 2004), presumably of Andean type because of some Precambrian inheritance in zircons of some of these granitoids (Fig. 9).

Implications for exhumation of the Inner Mongolia Palaeo-uplift

Aluminium-in-hornblende barometry results indicate that the Longhua, Daguangding and Boluonuo plutons were emplaced at depths of 15.7–18.7 km (Zhang *et al.* 2006). Because some of these Carboniferous plutons are unconformably overlain by Early Jurassic to Cretaceous volcanic and sedimentary rocks (HBGMR 1989), at least some of them were already exposed at the surface prior to the early Jurassic. We infer that the exhumation of the Inner Mongolia Palaeo-uplift was at least 15.7 km; this includes the removal of Archaean–Palaeoproterozoic basement rocks,

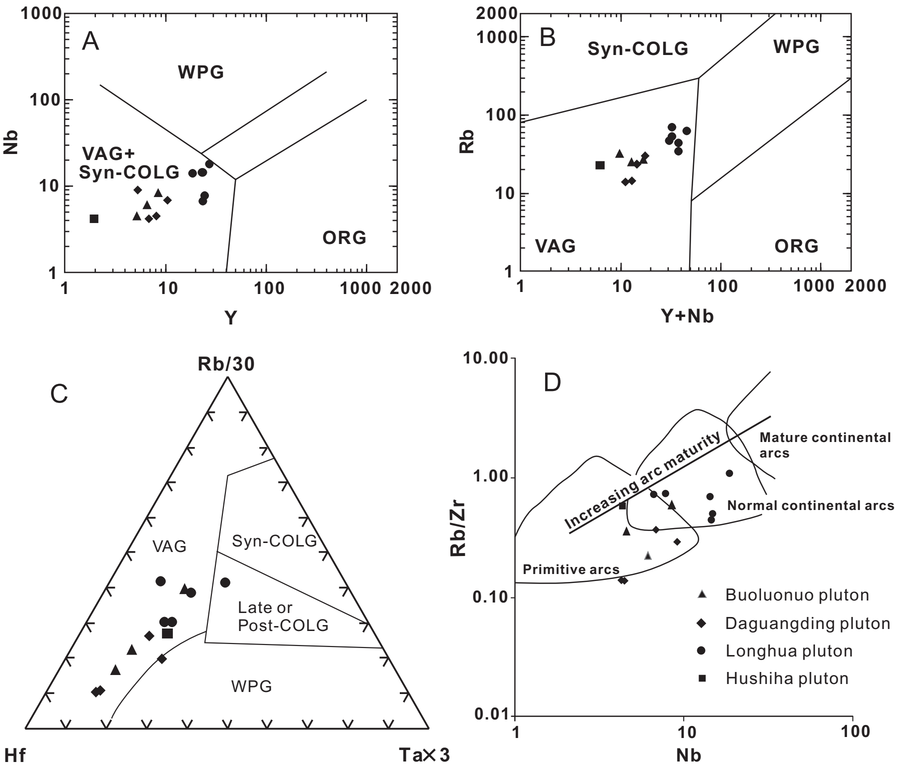

Fig. 8. Trace element discrimination diagram of the tectonic setting and arc maturity. (**a**) Nb v. Y discrimination diagram for granitoids from Pearce *et al*. (1984); (**b**) Rb v. Y + Nb discrimination diagram for granitoids from Pearce *et al*. (1984); (**c**) (Rb/30)–Hf–(Ta × 3) discrimination diagram for granitoids from Harris *et al*. (1986); (**d**) trace element arc maturity indicators after Brown *et al*. (1984). VAG, volcanic-arc granitoids; ORG, ocean-ridge granitoids; WPG, within-plate granitoids; Syn-COLG, syn-collisional granitoids; Late or Post-COLG, late or post-collisional granitoids.

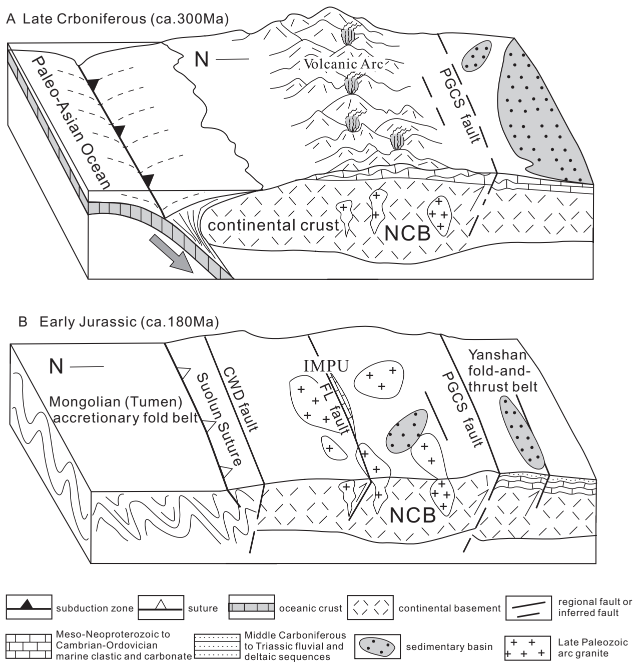

Fig. 9. Three-dimensional schematic illustrations of tectonic reconstruction of the northern margin of the North China block during the late Carboniferous (*c*. 300 Ma) and early Jurassic (*c*. 180 Ma). (**a**) In late Carboniferous time (*c*. 300 Ma), the Palaeo-Asian oceanic plate subducted beneath the northern margin of the North China block; an Andean-style continental arc developed and probably some volcanic ash was transported by wind and streams and redeposited in southern basins; arc granite plutons were emplaced at a depth of *c*. 15–18 km; Meso-Neoproterozoic marine clastic and carbonate, and probably Cambrian–Ordovician marine clastic and carbonate and late Carboniferous volcanic rocks, once existed in the Inner Mongolia Palaeo-uplift. (**b**) In early Jurassic time (*c*. 180 Ma), arc granite plutons were exposed at the surface and were unconformably overlain by early Jurassic volcanic and sedimentary rocks; Meso-Neoproterozoic, Cambrian–Ordovician marine clastic and carbonate and late Carboniferous volcanic rocks within the Inner Mongolia Palaeo-uplift were entirely eroded, except for some Mesoproterozoic quartzite along the Fengning–Longhua fault. Age of early Jurassic rock is from Davis *et al*. (2001). NCB, North China block; IMPU, Inner Mongolia Palaeo-uplift; FL fault, Fengning–Longhua fault; PGCS fault, Pingquan–Gubeikou–Chicheng–Shangyi fault; CWD fault, Chifeng–Weichang–Duolun fault. Illustrations are not to scale.

Meso-Neoproterozoic sedimentary rocks, and probably some early Palaeozoic, late Palaeozoic or Early–Middle Triassic sedimentary and volcanic rocks between the late Carboniferous and the early Jurassic. A Mesoproterozoic quartzite along the Fengning–Longhua fault is presumably the remainder of eroded strata within the Inner Mongolia Palaeo-uplift (Fig. 9). This strong exhumation explains the absence of Palaeozoic–early Mesozoic strata and Carboniferous continental arc volcanic rocks in the Inner Mongolia Palaeo-uplift, which can reasonably be considered to be the mid-crustal ‘root’ of a deeply eroded late Palaeozoic Andean-style arc along the northern margin of the North China block.

Timing of final collision of the southern Mongolia composite terranes and the North China block

The time of final closure of the Palaeo-Asian Ocean and collision between the southern Mongolia composite terranes and the North

China block has long been controversial: latest Silurian to Devonian (e.g. Yue *et al*. 2001), middle to late Devonian (e.g. Tang 1990; Xu & Chen 1997), late Devonian to early Carboniferous (e.g. Hong *et al*. 1995; Shao & Zhan 1998), late Carbounferous (e.g. Dobretsov *et al*. 1995), early Permian (e.g. Wang *et al*. 1999), late Permian (e.g. Hsu *et al*. 1991; Wang & Mo 1995; Sengör & Natal'in 1996; Wang 1996; Yin & Nie 1996; Xiao *et al*. 2003), Permo-Triassic (Chen *et al*. 2000), Middle–Late Triassic (e.g. Dorjnamjaa *et al*. 1993; Badarch & Orolmma 1998), or even Cretaceous (Nozaka & Liu 2002). The existence of late Carboniferous magmatic arc granitoids on the northern margin of the North China block and latest Carboniferous–earliest Permian tuff and possible volcanic activity indicates that the Palaeo-Asian Ocean still existed during the latest Carboniferous–earliest Permian time, and the final collision between the southern Mongolia composite terranes and the North China block occurred later than *c*. 290 Ma. Combined with the newly discovered radiolarians in an argillite bed of the Middle Permian Zhesi Formation in Zhesi and Xilinhot, Inner Mongolia (Shang 2004), we suggest that the Palaeo-Asian Ocean was not closed until the late Permian (Guadalupian, Shang 2004), which supports the Permian–Triassic collision model of two active continental margins of Xiao *et al*. (2003).

Conclusions

Variably foliated plutons on the northern margin of the North China block, which were once assigned to the Precambrian crystalline basement, have now been identified as being Carboniferous in age. The Longhua, Daguangding and Boluonuo quartz diorites and the Hushiha granodiorite crystallized at 311 ± 2 Ma, 324 ± 6 Ma, 302 ± 4 Ma and 310 ± 5 Ma, respectively. These calc-alkaline, I-type plutons formed in a continental magmatic arc of Andean type during southward subduction of the Palaeo-Asian oceanic crust beneath the North China block.

The Inner Mongolia Palaeo-uplift was not always an uplifted domain between the Neoproterozoic and the early Triassic. The present Inner Mongolia Palaeo-uplift is the consequence of major uplift and erosion between the Carboniferous and the Early Mesozoic. Exhumation of the deep (>15.7 km) plutons prior to early Jurassic time was accompanied by the removal of higher levels of Precambrian basement and supracrustal rocks of the late Palaeozoic Andean-style continental arc. The Inner Mongolia Palaeo-uplift along the northern margin of the North China block is therefore a deeply eroded mid-crustal 'root' of a late Palaeozoic Andean-style continental arc.

We thank B. M. Jahn, A. Yin, D. Hong, T. Wang, S. Liu, S. Cui, J. Li, Y. Yao, Y. Ma and J. Yang for critical comments and helpful suggestions, and D. Liu for considerable help during the SHRIMP analyses. Earlier versions of the manuscript were significantly improved by thoughtful reviews by A. Kröner, B. F. Windley, S. A. Wilde, C. Miller, M. Reid and W. M. White. We are grateful to G. A. Davis and W. J. Xiao for constructive and helpful reviews, and to M. Whitehouse for comments and editorial handling. This research was financially supported by grants from the National Natural Science Foundation of China (grants 40132020 to Y.Z. and 40402018 to S.H.Z.), the Ministry of Science and Technology of China (grant 2006CB403500) and China Geological Survey (grant 20021022 to Y.Z.).

References

Badarch, G. & Orolmma, D. 1998. Overview of the geology and tectonic evolution of southern Mongolia. *Mongolia Geoscientist*, **10**, 10–16.

Black, L.P., Kamo, S.L., Allen, C.M., Aleinikoff, J.N., Davis, D.W., Korsch, R.J. & Foudoulis, C. 2003. TEMORA 1: a new zircon standard for Phanerozoic U–Pb geochronology. *Chemical Geology*, **200**, 155–170.

Briqueu, L., Bougault, H. & Joron, J.L. 1984. Quantification of Nb, Ta, Ti and V anomalies in magmas associated with subduction zones: petrogenetic implications. *Earth and Planetary Science Letters*, **68**, 297–308.

Brown, C.G., Thorpe, R.S. & Webb, P.C. 1984. The geochemical characteristics of granitoids in contrasting arcs and comments on magma sources. *Journal of the Geological Society, London*, **141**, 411–426.

Chen, B., Jahn, B.M., Wilde, S. & Xu, B. 2000. Two contrasting Paleozoic magmatic belts in northern Inner Mongolia, China: petrogenesis and tectonic implications. *Tectonophysics*, **328**, 157–182.

Cope, T.D., Ritts, B.D., Darby, B.J., Fildani, A. & Graham, S.A. 2005. Late Paleozoic sedimentation on the northern margin of the North China block: implications for regional tectonics and climate change. *International Geology Review*, **47**, 270–296.

Cui, S. & Wu, Z. 1997. On the Mesozoic and Cenozoic intracontinental orogenesis of the Yanshan area, China. *In:* Zheng, Y.D. (ed.) *Proceedings of the 30th International Geological Congress*. VSP, Utrecht, 277–292.

Davis, G.A., Zheng, Y., Wang, C., Darby, B.J., Zhang, C. & Gehrels, G. 2001. Mesozoic tectonic evolution of the Yanshan fold and thrust belt, with emphasis on Hebei and Liaoning Provinces, Northern China. *In:* Hendrix, M.S. & Davis, G.A. (eds) *Paleozoic and Mesozoic Tectonic Evolution of Central and Eastern Asia*. Geological Society of America, Memoirs, **194**, 171–197.

Defant, M.J. & Drummond, M.S. 1990. Derivation of some modern arc magmas by melting of young subducted lithosphere. *Nature*, **347**, 662–665.

Dobretsov, N.L., Berzin, N.A. & Buslov, M.M. 1995. Opening and tectonic evolution of the Paleo-Asian Ocean. *International Geology Review*, **37**, 335–360.

Dorjnamjaa, D., Badarch, G. & Orolmma, D. 1993. The geodynamic evolution of the mobile fold belts of the territory of Mongolia. *In:* Coleman, R.G. (ed.) *Reconstruction of the Paleo-Asian Ocean. Proceedings of the 29th International Geological Congress*. VSP, Utrecht, 63–76.

Drummond, M.S. & Defant, M.J. 1990. A model for trondhjemite–tonalite–dacite genesis and crustal growth via slab melting: Archean to modern comparisons. *Journal of Geophysical Research*, **95**, 21503–21521.

Drummond, M.S., Defant, M.J. & Kepezhinskas, P.K. 1996. Petrogenesis of slab-derived trondhjemite–tonalite–dacite/adakite magmas. *Transactions of the Royal Society of Edinburgh*, **87**, 205–215.

Evensen, N.M., Hamilton, P.J. & O'Nions, R.K. 1978. Rare earth element abundances in chondritic meteorites. *Geochimica et Cosmochimica Acta*, **42**, 1199–1212.

Gorton, M.P. & Schandl, E. 2000. From continents to island arcs: a geochemical index of tectonic setting for arc-related and within-plate felsic to intermediate volcanic rocks. *Canadian Mineralogist*, **38**, 1065–1073.

Harris, N.B.W., Pearce, J.A. & Tindle, A.G. 1986. Geochemical characteristics of collision-zone magmatism. *In:* Coward, M.P. & Ries, A.C. (eds) *Collision Tectonics*. Geological Society of America, Special Papers, **9**, 67–81.

Harvey, P.K. 1989. Automated X-ray fluorescence in geochemical exploration. *In:* Ahmedali, S.T. (ed.) *X-ray Fluorescence Analysis in the Geological Sciences, Advances in Methodology*. Geological Association of Canada, Short Courses, **7**, 221–257.

HBGMR (Hebei Bureau of Geology and Mineral Resources) 1974. *Geological map of Chengde, scale 1:200 000* [in Chinese].

HBGMR (Hebei Bureau of Geology and Mineral Resources) 1988. *Geological map of Boluonuo, Shirengou and Hongqi, scale 1:50 000* [in Chinese].

HBGMR (Hebei Bureau of Geology and Mineral Resources) 1989. *Regional geology of Hebei Province, Beijing Municipality and Tianjin Municipality*. Geological Publishing House, Beijing [in Chinese with English abstract].

HBGMR (Hebei Bureau of Geology and Mineral Resources) 1994a. *Geological map of Hanmaying, scale 1:50 000* [in Chinese].

HBGMR (Hebei Bureau of Geology and Mineral Resources) 1994b. *Geological map of Longhua County, scale 1:50 000* [in Chinese].

Heubeck, C. 2001. Assembly of central Asia during the middle and late Paleozoic. *In:* Hendrix, M.S. & Davis, G.A. (eds) *Paleozoic and Mesozoic Tectonic Evolution of Central and Eastern Asia*. Geological Society of America, Memoirs, **194**, 1–22.

Hong, D., Huang, H., Xiao, Y., Xu, H. & Jin, M. 1995. Permian alkaline granites in central Inner Mongolia and their geodynamic significance. *Acta Geologica Sinica*, **8**, 27–39.

Hsu, K.J., Wang, Q., Li, J. & Hao, J. 1991. Geologic evolution of the Neimonides: a working hypothesis. *Eclogae Geologicae Helvetiae*, **84**, 1–31.

Huang, T.K. 1945. *On major tectonic forms of China*. Geological Memoirs (Series A), National Geological Survey of China, **20**.

Jahn, B.M., Wu, F.Y. & Chen, B. 2000. Granitoids of the Central Asian Orogenic Belt and continental growth in the Phanerozoic. *Transactions of the Royal Society of Edinburgh: Earth Sciences*, **91**, 181–193.

Jia, B., Zhou, A. & Gu, D. 1999. Geochemistry and provenance analysis of Late Paleozoic volcanic event deposits in West Liaoning. *Acta Sedimentologica Sinica*, **17**, 473–477 [in Chinese with English abstract].

Kröner, A., Windley, B.F. & Khain, E.V. *et al.* 2004. Accretionary growth and crust-formation in the Central Asian Orogenic Belt during the Neoproterozoic (2) and Paleozoic and comparison with the present southwest Pacific. *Program with Abstracts of the 2004 International Basement Tectonics Association Conference, June 27–July 1, 2004, Oak Ridge, TN*. 78–80.

LBGMR (Liaoning Bureau of Geology and Mineral Resources) 1989. *Regional geology of Liaoning Province*. Geological Publishing House, Beijing [in Chinese with English abstract].

Ludwig, K.R. 1999. *User's Manual for Isoplot/Ex, Version 2.06: a Geochronological Toolkit for Microsoft Excel*. Berkeley Geochronology Center, Special Publications, **1a**.

Ludwig, K.R. 2001. *SQUID 1.02: a User's Manual*. Berkeley Geochronology Center, Special Publications, **2**.

Martin, H. 1999. Adakitic magmas: modern analogues of Archaean granitoids. *Lithos*, **46**, 411–429.

Martin, H., Smithies, R.H., Rapp, R., Moyen, J.F. & Champion, D. 2005. An overview of adakite, tonalite–trondhjemite–granodiorite (TTG), and sanukitoid: relationships and some implications for crustal evolution. *Lithos*, **79**, 1–24.

Nozaka, T. & Liu, Y. 2002. Petrology of the Hegenshan ophiolite and its implication for the tectonic evolution of northern China. *Earth and Planetary Science Letters*, **202**, 89–104.

(3) Pan, Y. 1996. Early Permian Bajiazi ultra-unit intrusive rock and its emplacement mechanism, Jianping area. *Liaoning Geology*, 284–292 [in Chinese with English abstract].

Pearce, J.A., Harris, N.B.W. & Tindle, A.G. 1984. Trace element discrimination diagrams for the tectonic interpretation of granitic rocks. *Journal of Petrology*, **25**, 956–983.

Peccerillo, A. & Taylor, S.R. 1976. Geochemistry of Eocene calc-alkaline volcanic rocks from the Kastamanonu area, Turkey. *Contributions to Mineralogy and Petrology*, **58**, 39–63.

Ren, J., Chen, T., Niu, B., Liu, Z. & Liu, F. 1990. *Tectonic evolution of the continental lithosphere and metallogeny in Eastern China and adjacent area*. Science Press, Beijing [in Chinese].

Robinson, P.T., Zhou, M.F., Hu, X.F., Reynolds, P., Bai, W. & Yang, J. 1999. Geochemical constraints on the origin of the Hegenshan Ophiolite, Inner Mongolia, China. *Journal of Asian Earth Sciences*, **17**, 423–442.

Rogers, G. & Hawkesworth, C.J. 1989. A geochemical traverse across the North Chilean Andes: evidence for crustal generation from the mantle wedge. *Earth and Planetary Science Letters*, **91**, 271–285.

Sajona, F.G., Maury, R.C., Bellon, H., Cotten, J. & Defant, M. 1996. High field strength element enrichment of Pliocene–Pleistocene island-arc basalts, Zamboanga Peninsula, Western Mindanao (Philippines). *Journal of Petrology*, **37**, 693–726.

Sengör, A.M.C. & Natal'in, B.A. 1996. Paleotectonics of Asia: fragments of a synthesis. *In:* Yin, A. & Harrison, T.M. (eds) *Tectonic Evolution of Asia*. Cambridge University Press, Cambridge, 486–640.

Sengör, A.M.C., Natal'in, B.A. & Burtman, V.S. 1993. Evolution of the Altaid tectonic collage and Paleozoic crustal growth in Eurasia. *Nature*, **364**, 299–307.

Shang, Q.H. 2004. Occurrences of Permian radiolarians in central and eastern Nei Mongol (Inner Mongolia) and their geological significance to the Northern China Orogen. *Chinese Science Bulletin*, **49**(24), 2613–2619.

Shao, J. & Zhan, L. 1998. North-east Asian terranes and Permian palaeogeography in Inner Mongolia, China. *Proceedings of the Royal Society of Victoria*, **110**, 317–321.

Shi, Y., Liu, D. & Zhang, Q. *et al.* 2004. SHRIMP dating of diorites and granites in southern Suzuoqi, Inner Mongolia. *Acta Geologica Sinica*, **78**(6), 789–799 [in Chinese with English abstract].

Smithies, R.H. 2000. The Archaean tonalite–trondhjemite–granodiorite (TTG) series is not an analogue of Cenozoic adakite. *Earth and Planetary Science Letters*, **182**, 115–125.

Song, H. 1999. Characteristics of Yanshan type intraplate orogenic belts and a discussion on its dynamics. *Earth Science Frontiers*, **6**, 309–316 [in Chinese with English abstract].

Sun, S.S. & McDonough, W.F. 1989. Chemical and isotopic systematics of oceanic basalts: implications for mantle composition and processes. *In:* Saunders, A.D. & Norry, M.J. (eds) *Magmatism in the Ocean Basins*. Geological Society, London, Special Publications, **42**, 313–345.

Tang, K. 1990. Tectonic development of Paleozoic fold belts at the north margin of the Sino-Korean craton. *Tectonics*, **9**, 249–260.

Taylor, S.R. & McLennan, S.M. 1985. *The Continental Crust: its Composition and Evolution*. Blackwell Scientific, Oxford.

Wang, H. & Mo, X. 1995. An outline of the tectonic evolution of China. *Episodes*, **18**, 6–16.

Wang, Q. & Liu, X.Y. 1986. Paleoplate tectonics between Cathaysia and Angaraland in Inner Mongolia of China. *Tectonics*, **5**, 1073–1088.

Wang, Y. 1996. *Tectonic evolutional processes of Inner Mongolia–Yanshan orogenic belt in eastern China during the Late Paleozoic–Mesozoic*. Geological Publishing House, Beijing [in Chinese with English summary].

Wang, Y., Fan, Z.Y., Fang, S. & Li, B.Y. 1999. Geological information (4) discovered and its plate tectonic significance on the northern bank of Xarmoron River. *Geology of Inner Mongolia*, 1, 6–28 [in Chinese with English abstract].

Williams, I.S. 1998. U–Th–Pb geochronology by ion microprobe. *In:* McKibben, M.A., Shanks, W.C. III & Ridley, W.I. (eds) *Applications of Microanalytical Techniques to Understanding Mineralizing Processes*. Reviews in Economic Geology, **7**, 1–35.

Xiao, W.J., Windley, B.F., Hao, J. & Zhai, M. 2003. Accretion leading to collision and the Permian Solonker suture, Inner Mongolia, China: termination of the central Asian orogenic belt. *Tectonics*, **22**, 1069, doi:10.1029/2002TC001484.

Xu, B. & Chen, B. 1997. Framework and evolution of the middle Paleozoic orogenic belt between Siberian and north China plates in northern Inner Mongolia. *Science in China (Series D)*, **40**, 463–479.

Yin, A. & Nie, S.Y. 1996. A Phanerozoic palinspastic reconstruction of China and its neighbouring regions. *In:* Yin, A. & Harrison, T.M. (eds) *Tectonic Evolution of Asia*. Cambridge University Press, Cambridge, 442–485.

Yue, Y.J., Liou, J.G. & Graham, S.A. 2001. Tectonic correlation of Beishan and Inner Mongolia orogens and its implications for the palinspastic reconstruction of North China. *In:* Hendrix, M.S. & Davis, G.A. (eds) *Paleozoic and Mesozoic Tectonic Evolution of Central and Eastern Asia*. Geological Society of America, Memoirs, **194**, 101–116.

Zhang, S.H. 2004. *The Late Paleozoic–Early Mesozoic tectonomagmatic activities in the eastern segment of the Inner Mongolia Paleo-uplift in the Yanshan tectonic belt and their geological significance*. PhD thesis, Chinese Academy of Geological Sciences, Beijing [in Chinese with English abstract].

Zhang, S.H., Zhao, Y. & Song, B. 2006. Hornblende therobarometry of the Carboniferous granitoids from the Inner Mongolia Paleo-uplift: implications for the geotectonic evolution of the northern margin of North China block. *Mineralogy and Petrology*, **87**, 123–141.

Zhang, Y., Wu, F., Wilde, S.A., Zhai, M., Lu, X. & Sun, D. 2004. Zircon U–Pb ages and tectonic implications of 'Early Paleozoic' granitoids at Yanbian, Jilin Province, northeast China. *Island Arc*, **13**, 484–505.

Zhong, R., Sun, S., Chen, F. & Fu, Z. 1995. The discovery of rhyo-tuffite in the Taiyuan Formation and stratigraphic correlation of the Daqingshan and Datong coalfields. *Acta Geoscientia Sinica*, **16**, 291–301 [in Chinese with English abstract].

Zhou, A., Jia, B., Ma, M. & Zhang, H. 2001. The whole sequences of volcanic event deposits on the north margin of the North China plate and their features. *Geological Review*, **47**, 175–183 [in Chinese with English abstract].

Zhou, M.F., Yan, D., Kennedy, A.K., Li, Y. & Ding, J. 2002. SHRIMP U–Pb zircon geochronological and geochemical evidence for Neoproterozoic arc-magmatism along the western margin of the Yangtze Block, South China. *Earth and Planetary Science Letters*, **196**, 51–67.

Received 5 January 2006; revised typescript accepted 1 August 2006.
Scientific editing by Martin Whitehouse

1 Should Peking be changed to Beijing?
2 Kröner et al. - please give editor/s, and publisher's name + town if known.
3 Pan - please give volume number if there is one.
4 Wang et al. 1999 - please confirm changes in title are OK.